

A Robust Multiplicative Watermark Detector for Color Images in Sparse Domain

H. Sadreazami, *Student Member, IEEE*, M. Omair Ahmad, *Fellow, IEEE*, and M. N. S. Swamy, *Fellow, IEEE*

Abstract—In recent years, digital watermarking has facilitated the protection of copyright information through embedding hidden information into the digital content. In this brief, for the first time, a blind multichannel multiplicative color image watermarking scheme in the sparse domain is proposed. In order to take into account the cross correlation between the coefficients of the color bands in the sparse domain, a statistical model based on the multivariate Cauchy distribution is used. The statistical model is then used to derive an efficient closed-form decision rule for the watermark detector. Experimental results and theoretical analysis are presented to validate the proposed watermark detector. The performance of the proposed detector is compared with that of the other detectors. The results demonstrate the improved detection rate and high robustness against the commonly used attacks such as JPEG compression, salt and pepper noise, median filtering, and Gaussian noise.

Index Terms—Color image watermarking, contourlet transform, multiplicative watermark, multivariate Cauchy distribution, watermark detection.

I. INTRODUCTION

DIGITAL image watermarking as a tool for copyright protection has attracted a lot of attention in the past few years. Most of the image watermarking schemes have focused on grayscale images. The generalization of such schemes for color images is feasible by marking the luminance channel in the luminance/chrominance, i.e., Yuv , domain or through marking each channel separately. However, it has been shown that the dependencies between the RGB channels can remarkably improve the performance of watermark detection [1]. In [1], a watermarking technique has been proposed in the discrete cosine transform domain in which the dependencies of the RGB channels have been taken into account by defining a global correlation measure. In [2], a quaternion Fourier transform (QFT)-based nonblind color image watermarking technique has been proposed. However, by ignoring pure quaternion precondition, its performance is not satisfactory both in terms of visual quality and extracting the watermark bits. In [3], a color image watermarking scheme in the QFT domain based on the least square support vector machine (LS-SVM) combined

with pseudo-Zernike moments has been proposed. As stated by the authors in [3], the drawback of this work is the high computation time required for LS-SVM training and to calculate the pseudo-Zernike moments. In [4], all the four components of the QFT have been considered for watermark embedding, which is at the expense of a more complex scheme than those in [2] and [3]. In [5], a genetic algorithm has been used to adaptively embed the watermark bits in a nonblind color image watermarking scheme. As stated by the authors, this scheme suffers from a heavy load of computations strictly connected with the estimation of the quaternion radial moments. In [6], a wavelet-based watermarking scheme for color images has been proposed through visual masking in the Yuv domain. However, it does not take the color information into account by ignoring the chrominance components. In [7], the histogram bin shifting technique has been used for reversible watermarking of the color images. However, the performance of this algorithm is not satisfactory in the RGB color space.

In many watermarking schemes in the transform domain, a decision rule has been made by a binary hypothesis test to verify the presence or absence of the hidden information. It has been shown that the effectiveness of a watermark detector highly depends on the modeling of the transform-domain coefficients [8], [9]. In [9], the Weibull density function has been used to model the discrete Fourier transform coefficients of color images. In [10], a multivariate power-exponential (MPE) distribution has been proposed to capture the wavelet subband statistics and dependencies across RGB channels in an additive color image watermarking scheme. However, the proposed detector in [10] is not robust when the watermark is low powered or the watermarked image is under attack.

In view of this and the fact that none of the existing works in the literature have considered a multiplicative watermarking scheme for color images, in this brief, for the first time, we propose a multichannel multiplicative watermark detector for color images that aims at improving the watermark detection rate. The proposed detector is based on the multivariate Cauchy distribution. A Bayesian log-likelihood ratio test is employed to derive an efficient closed-form expression for the test statistics. The performance of the proposed detector is evaluated by obtaining the receiver operating characteristic (ROC) curves. The robustness of the proposed watermarking scheme is examined when the watermarked images undergo JPEG compression, Gaussian noise, median filtering, and salt and pepper noise.

II. WATERMARKING SCHEME

To embed the watermark bits, the original RGB color channels are separately decomposed into a number of subbands

Manuscript received June 12, 2015; accepted August 9, 2015. Date of publication August 17, 2015; date of current version November 25, 2015. This work was supported in part by the Natural Sciences and Engineering Research Council of Canada and in part by the Regroupement Stratégique en Microélectronique du Québec (ReSMiQ). This brief was recommended by Associate Editor C. Shing-chow.

The authors are with the Centre for Signal Processing and Communications, Concordia University, Montreal, QC H3G 1M8, Canada (e-mail: h_sadrea@encs.concordia.ca; omair@encs.concordia.ca; swamy@encs.concordia.ca).

Color versions of one or more of the figures in this brief are available online at <http://ieeexplore.ieee.org>.

Digital Object Identifier 10.1109/TCSIL.2015.2468995

by using the contourlet transform with the highest sparsity among other transforms [11]. It is known that the watermark should be inserted into the significant features of an image in order to increase the robustness of the watermark [12]. In view of this, the directional subband with the highest entropy in the second scale of each channel is chosen for embedding purposes. The contourlet coefficients of the selected subband are modified as $\mathbf{y} = \mathbf{x}(1 + \zeta\mathbf{w})$, where $\mathbf{x} = [x_1, x_2, x_3]$ and $\mathbf{y} = [y_1, y_2, y_3]$ are the original and marked coefficients of the RGB channels, $\mathbf{w} = [w_1, w_2, w_3]$ is the watermark of size $N \times 3$, and ζ is a positive watermark weighing factor. The watermark is generated using a direct-sequence spread spectrum technique, wherein the watermark is generated using a pseudorandom sequence generator that has an authentication key as its initial value. This pseudorandom sequence spreads the spectrum of the watermark signal over many coefficients, making it difficult to be detected. The watermarked contourlet coefficients are then inversely transformed to obtain the watermarked image. To detect the presence of the watermark in the receiver, the signal statistics is taken into account via modeling the contourlet coefficients of RGB color channels by the multivariate Cauchy distribution. The Cauchy model has been shown to accurately fit the histogram of the contourlet coefficients of images [8]. To design the watermark detector, we employ a Bayesian log-likelihood ratio test, which can be reduced to a binary hypothesis test as

$$\begin{aligned} H_1 : \mathbf{y} &= \mathbf{x}(1 + \zeta\mathbf{w}) \text{ (watermarked)} \\ H_0 : \mathbf{y} &= \mathbf{x} \text{ (not - watermarked)}. \end{aligned} \quad (1)$$

Hypotheses H_1 and H_0 correspond to whether or not the contourlet coefficients are watermarked by the sequence \mathbf{w} , respectively. The decision rule is then defined as the log-likelihood ratio given by

$$\Lambda_{\text{det}} = \ln \left(\frac{f_{\mathbf{Y}}(\mathbf{y}|H_1)}{f_{\mathbf{Y}}(\mathbf{y}|H_0)} \right) \begin{array}{l} > \\ < \\ \end{array} \begin{array}{l} H_1 \\ \tau \\ H_0 \end{array} \quad (2)$$

where τ is the decision threshold and

$$\begin{aligned} f_{\mathbf{Y}}(\mathbf{y}|H_0) &= f_{X_1, X_2, X_3}(y_1, y_2, y_3) \\ f_{\mathbf{Y}}(\mathbf{y}|H_1) &= \frac{f_{X_1, X_2, X_3} \left(\frac{y_1}{1+\zeta w_1}, \frac{y_2}{1+\zeta w_2}, \frac{y_3}{1+\zeta w_3} \right)}{(1 + \zeta w_1)(1 + \zeta w_2)(1 + \zeta w_3)}. \end{aligned} \quad (3)$$

The detector is supposed to choose between H_1 and H_0 based on the received image coefficients \mathbf{y} . Then, by assuming the independence of the observations, the log-likelihood ratio becomes

$$\begin{aligned} \Lambda_{\text{det}} &= \sum_{i=1}^N \ln \left(\frac{P \left(\frac{y_{1i}}{1+\zeta w_{1i}}, \frac{y_{2i}}{1+\zeta w_{2i}}, \frac{y_{3i}}{1+\zeta w_{3i}} \right)}{(1 + \zeta w_{1i})(1 + \zeta w_{2i})(1 + \zeta w_{3i}) P(y_{1i}, y_{2i}, y_{3i})} \right). \end{aligned} \quad (4)$$

To take into account the information carried out by all the three color channels, the data \mathbf{x} are modeled by the multivariate Cauchy distribution given by

$$f_{\mathbf{X}}(\mathbf{x} : n, \Sigma) = \frac{\Gamma \left(\frac{n+1}{2} \right)}{\Gamma \left(\frac{1}{2} \right) \pi^{\frac{1}{2}} |\Sigma|^{\frac{1}{2}} [1 + \mathbf{x}^T \Sigma^{-1} \mathbf{x}]^{\frac{n+1}{2}}} \quad (5)$$

where $\Gamma(\cdot)$ is the gamma function, and Σ is the covariance matrix of size $n \times n$. Thus, the log-likelihood ratio for the multivariate Cauchy distribution is obtained as

$$\begin{aligned} \Lambda_{\text{det}} &= \sum_{i=1}^N \ln \left(\frac{1 + \mathbf{y}_i^T \Sigma^{-1} \mathbf{y}_i}{1 + \mathbf{z}_i^T \Sigma^{-1} \mathbf{z}_i} \right)^2 \\ &+ \sum_{i=1}^N \ln \left| \frac{1}{(1 + \zeta w_{1i})(1 + \zeta w_{2i})(1 + \zeta w_{3i})} \right| \end{aligned} \quad (6)$$

where

$$\mathbf{z} = \left[\frac{y_1}{1 + \zeta w_1}, \frac{y_2}{1 + \zeta w_2}, \frac{y_3}{1 + \zeta w_3} \right]. \quad (7)$$

The log-likelihood ratio can be seen as a superposition of N statistically independent random variables. Thus, according to the central limit theorem, the log-likelihood ratio follows a Gaussian distribution under each hypothesis. The mean and variance of each of the Gaussian distributions can be estimated from the empirical data and are given by (μ_0, μ_1) and (σ_0^2, σ_1^2) for H_0 and H_1 , respectively. After some mathematical manipulations on (6), the theoretical mean and variance of the log-likelihood ratio under H_0 can be shown to be (see the Appendix)

$$\begin{aligned} \mu_0 &= \frac{-3}{2} [\ln(1 + \zeta) + \ln(1 - \zeta)] \\ &+ \sum_{i=1}^N \ln \frac{(1 + \mathbf{y}_i^T \Sigma^{-1} \mathbf{y}_i)^2}{\left(1 + \frac{\mathbf{y}_i^T \Sigma^{-1} \mathbf{y}_i}{(1+\zeta)^2}\right) \left(1 + \frac{\mathbf{y}_i^T \Sigma^{-1} \mathbf{y}_i}{(1-\zeta)^2}\right)} \end{aligned} \quad (8)$$

$$\sigma_0^2 = \sum_{i=1}^N \left(\frac{3}{2} \ln \frac{1 + \zeta}{1 - \zeta} + \ln \frac{1 + \frac{\mathbf{y}_i^T \Sigma^{-1} \mathbf{y}_i}{(1-\zeta)^2}}{1 + \frac{\mathbf{y}_i^T \Sigma^{-1} \mathbf{y}_i}{(1+\zeta)^2}} \right)^2. \quad (9)$$

It can be also shown that $\mu_1 = -\mu_0$ and $\sigma_1^2 = \sigma_0^2$. Having found the mean and variance of the log-likelihood ratio under both hypotheses, the probabilities of false alarm and detection can be estimated as

$$\begin{aligned} P_{\text{fa}} &= Q \left(\frac{\tau - \mu_0}{\sigma_0} \right) \\ P_{\text{det}} &= Q \left(\frac{\tau - \mu_1}{\sigma_1} \right) \end{aligned} \quad (10)$$

where $Q(x) = (1/\sqrt{2\pi}) \int_x^\infty e^{-z^2/2} dz$. The ROC curves are obtained by relating the probability of detection P_{det} to a predefined probability of false alarm P_{fa} in a Neyman–Pearson sense, given in [13], i.e., $P_{\text{det}} = Q(Q^{-1}(P_{\text{fa}}) - (2\mu_1/\sigma_1))$. It should

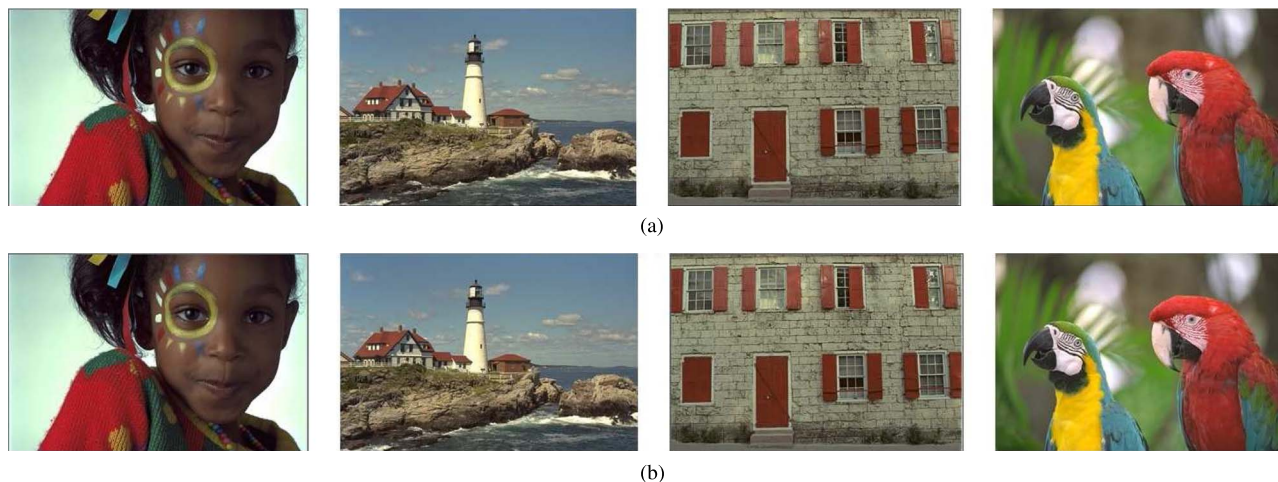


Fig. 1. (a) Original and (b) watermarked Kodak images, from left to right: *Girl*, *Headlight*, *Window*, and *Parrots*, with PSNR values of 68.08, 64.16, 63.45, and 69.57 dB, respectively.

be noted that the probability of detection needs to be kept at a high level for a predefined rate of false alarm to increase the reliability of detection. In order to estimate the covariance matrix Σ from the observation, we resort to the maximum-likelihood estimation via the expectation-maximization algorithm proposed in [14].

III. SIMULATION RESULTS

Experiments are performed using a set of color images, including Kodak and standard (for example, Lena and Baboon) images, each resized to 256 pixels \times 256 pixels. The RGB color channels are first decomposed using the contourlet transform into two scales and eight directions in each scale. The watermark bits are embedded in each color channel in a multiplicative manner resulting in higher robustness with respect to single-channel [1], [9] or additive watermarking algorithms [10]. In Fig. 1, some of the original and watermarked Kodak images are illustrated. The images are indistinguishable with high peak signal-to-noise-ratio (PSNR) values obtained by averaging over 10 runs with 100 different watermark sequences and a watermark weighting factor $\zeta = 0.5$, thus showing the effectiveness of the proposed scheme in terms of the invisibility of the watermark.

In order to evaluate the performance of the proposed watermark detector, we examine the closeness of the theoretical and experimental ROC curves for the proposed detector. The experimental results are obtained by using a Monte Carlo simulation with 1000 randomly generated watermark sequences. Fig. 2 shows the experimental and theoretical ROC curves averaged over a set of color images. It is seen from this figure that the theoretical ROC curves are close to the empirical ones indicating the accuracy of the closed-form expressions in (8) and (9) for the mean and variance of the log-likelihood ratio.

We then compare the detection performance of the proposed blind watermark detector to that of the RGB joint correlator [1], luminance-GG/Cauchy [9], and RGB-MPE [10]. Fig. 3 shows the ROC curves of various detectors averaged over a set of color images. It is seen from this figure that the proposed

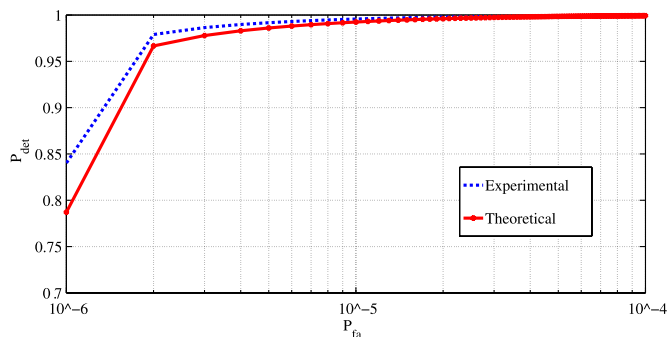


Fig. 2. (Dashed) Experimental and (solid) theoretical ROC curves averaged over a set of color images obtained using the proposed detector.

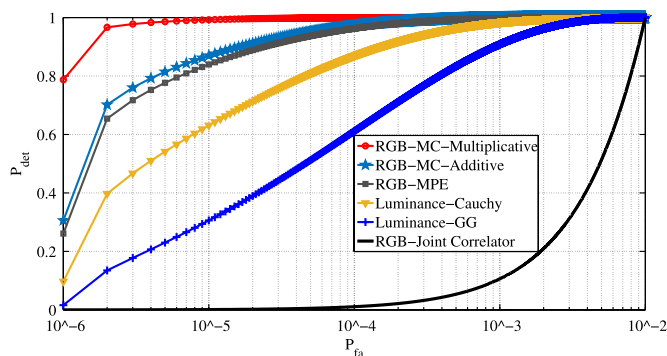


Fig. 3. ROC curve obtained using the proposed detector (multiplicative and additive) and that of the RGB joint correlator [1], luminance-GG/Cauchy [9], and RGB-MPE [10].

multiplicative watermark detector yields a performance that is substantially better than that of the other detectors as evidenced by a higher probability of detection for any given value of false alarm probability. It is also shown that the proposed multiplicative watermark detector provides a 15% gain over its additive counterpart.

The performances of the proposed watermark detector against two of the commonly used attacks, namely, JPEG compression and additive white Gaussian noise (AWGN), are

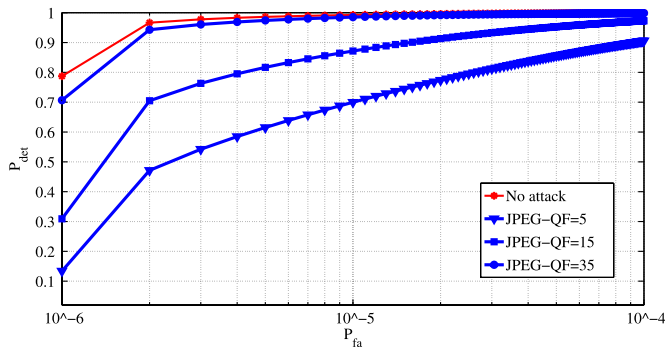


Fig. 4. ROC curves obtained using the proposed detector averaged over a set of color images when the watermarked images are JPEG compressed with various QFs.

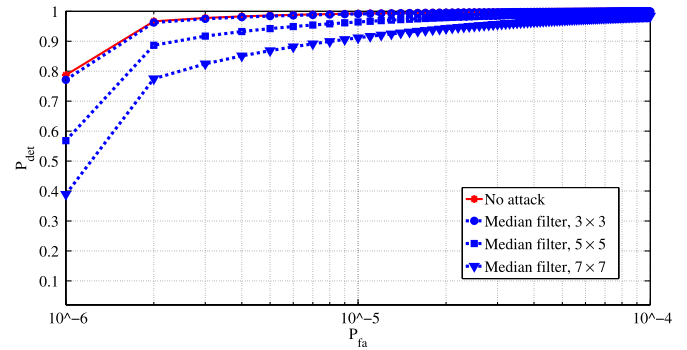


Fig. 6. ROC curves obtained using the proposed detector averaged over a set of color images when the watermarked images undergo median filtering with masks of various sizes.

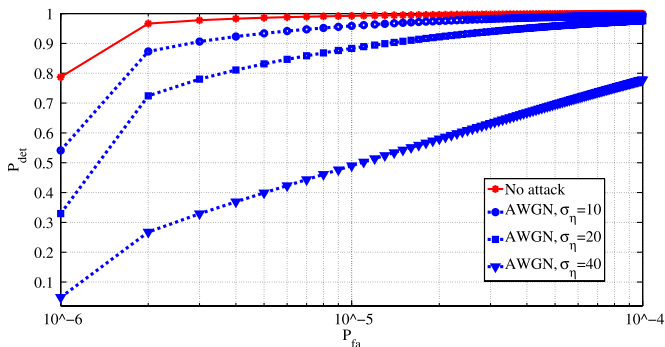


Fig. 5. ROC curves obtained using the proposed detector averaged over a set of color images when Gaussian noise with various σ_η is added to the watermarked images.

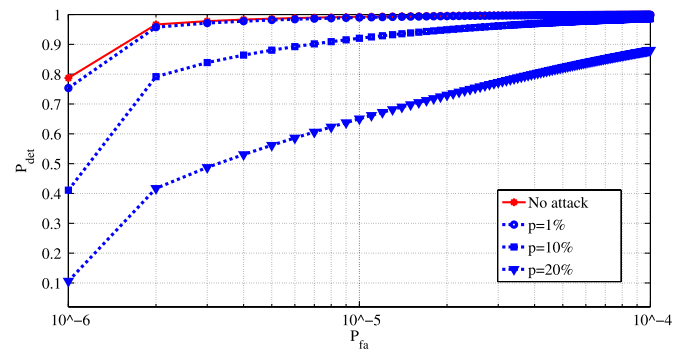


Fig. 7. ROC curves obtained using the proposed detector when the watermarked images are contaminated by salt and pepper noise with various probability of noisy pixels. p denotes the percentage of corrupted pixels.

then examined. Fig. 4 shows the ROC curves obtained using the proposed watermark detector averaged over a set of color images when the watermarked images are JPEG compressed with quality factor (QF) = 5, 15, and 35. It is seen from this figure that the proposed detector is highly robust against JPEG compression attack. More specifically, the detector is capable of detecting the presence of the watermark with the highest possible detection rate for a given P_{fa} when $QF > 35$. To study the robustness against noise, the watermarked images are corrupted by AWGN with standard derivation σ_η varying from 0 to 40. Fig. 5 shows the averaged ROC curves obtained using the proposed detector when the watermarked images are contaminated by Gaussian noise. It is seen from this figure that the proposed detector is highly robust against AWGN even under high-strength noise, i.e., $\sigma_\eta = 40$. Fig. 6 shows the ROC curves obtained using the proposed watermark detector when the watermarked images undergo median filtering with mask of sizes 3×3 , 5×5 , and 7×7 . From this figure, it is seen that the proposed detector is highly robust against median filtering. Fig. 7 shows the ROC curves averaged over a set of images when the watermarked images are contaminated by salt and pepper noise with equal probability. It is seen from this figure that the proposed watermark detector is robust against salt and pepper noise, particularly when the noise levels are less than 10%.

Unlike the QFT-based methods in [2]–[5] that are very complex, the proposed multiplicative detector is computationally

efficient since it requires 0.89- and 7.42-s CPU times averaged over a set of images on an Intel Core *i7* 2.93-GHz personal computer with 8-GB RAM for the cases of parameters that are predefined and estimated, respectively. In terms of capacity, it is known that, in the QFT-based methods, there is a symmetry constraint for embedding the watermark bits; this impacts their performance not only in terms of the capacity but also in terms of invisibility and robustness [4]. However, the proposed watermarking scheme is capable of fully employing the maximum possible capacity. In terms of the PSNR value of the watermarked images, the proposed scheme provides higher PSNR values for the watermarked images. For example, the PSNR values for one of the test images, i.e., *Lena* image of sizes 256×256 and 512×512 , are 53.84 and 64.21 dB, respectively, whereas the PSNR values given in [2], [3], [4] and [5] are 30 dB for the image of size 512×480 , 36.10 dB for the image of size 256×256 , 37.71 dB for the image of size 512×512 , and 40.38 dB for the image of size 512×512 , respectively.

IV. CONCLUSION

In this brief, we have proposed a blind statistical multiplicative watermark detector in the sparse domain for watermarking of color images. To efficiently exploit the statistical dependencies between the color channels in designing the watermark detector, the sparse domain coefficients of the channels have been modeled by the multivariate Cauchy distribution.

Employing this model, the statistical watermark detector has been designed through the Bayesian log-likelihood ratio test based on which closed-form expressions for the mean and variance of the log-likelihood ratio have been derived. Experiments have been carried out using standard color images to evaluate the performance of the proposed watermark detector. It has been shown that the performance of the proposed multiplicative watermark detector for color images is substantially superior to that of the other detectors in terms of providing a higher detection rate. It has been also shown that the proposed detector is highly robust against common attacks such as JPEG compression, Gaussian noise, median filtering, and salt and pepper noise.

APPENDIX

MEAN AND VARIANCE OF THE LOG-LIKELIHOOD RATIO UNDER HYPOTHESES H_0 AND H_1

For the proposed multichannel multiplicative watermark detector, the log-likelihood ratio Λ_{det} is given by (6). Let $\Lambda_{\text{det}} = g_1(\mathbf{y}) + g_2(\mathbf{y})$, where

$$\begin{aligned} g_1(\mathbf{y}) &= -\ln|(1 + \zeta w_1)(1 + \zeta w_2)(1 + \zeta w_3)| \\ g_2(\mathbf{y}) &= \ln \left(\frac{1 + \mathbf{y}^T \Sigma^{-1} \mathbf{y}}{1 + \mathbf{z}^T \Sigma^{-1} \mathbf{z}} \right)^2. \end{aligned} \quad (\text{A.1})$$

It is known that, for large N , the log-likelihood ratio under both hypotheses can be approximated by Gaussian distributions with means (μ_0, μ_1) and variances (σ_0^2, σ_1^2) [13]. The mean and variance of the log-likelihood ratio under H_0 (i.e., $\mathbf{y}_i = \mathbf{x}_i$) can be obtained as

$$\begin{aligned} \mu_0 &= \mu(\Lambda_{\text{det}}; H_0) \\ &= \sum_{i=1}^N (\mu_{g_1} + \mu_{g_2}) \end{aligned} \quad (\text{A.2})$$

$$\begin{aligned} \sigma_0^2 &= \sigma^2(\Lambda_{\text{det}}; H_0) \\ &= \sum_{i=1}^N (\sigma_{g_1}^2 + \sigma_{g_2}^2 - 2\mu_{g_1 g_2} + 2\mu_{g_1} \mu_{g_2}). \end{aligned} \quad (\text{A.3})$$

We assume that the watermark sequence where $w_1 = w_2 = w_3$ is generated by a pseudorandom sequence taking values $+1$ and -1 with equal probability. Hence, μ_{g_1} and μ_{g_2} can be obtained as

$$\mu_{g_1} = \frac{-3}{2} (\ln(1 + \zeta) + \ln(1 - \zeta)) \quad (\text{A.4})$$

$$\mu_{g_2} = \ln \left(\frac{1 + \mathbf{y}^T \Sigma^{-1} \mathbf{y}}{1 + \frac{\mathbf{y}^T \Sigma^{-1} \mathbf{y}}{(1+\zeta)^2}} \right) + \ln \left(\frac{1 + \mathbf{y}^T \Sigma^{-1} \mathbf{y}}{1 + \frac{\mathbf{y}^T \Sigma^{-1} \mathbf{y}}{(1-\zeta)^2}} \right). \quad (\text{A.5})$$

Substituting (A.4) and (A.5) into (A.2) and after making some manipulations, we can establish (8). In order to find the variance

of the log-likelihood ratio under H_0 , given by (A.3), the various terms are found and are given by

$$\sigma_{g_1}^2 = E [g_1^2] - \mu_{g_1}^2 = \frac{9}{4} (\ln(1 + \zeta) + \ln(1 - \zeta))^2 \quad (\text{A.6})$$

$$\sigma_{g_2}^2 = E [g_2^2] - \mu_{g_2}^2 = \left(\ln \frac{1 + \frac{\mathbf{y}^T \Sigma^{-1} \mathbf{y}}{(1-\zeta)^2}}{1 + \frac{\mathbf{y}^T \Sigma^{-1} \mathbf{y}}{(1+\zeta)^2}} \right)^2 \quad (\text{A.7})$$

$$\begin{aligned} \mu_{g_1 g_2} &= -\frac{3}{2} \ln \left(\frac{1 + \mathbf{y}^T \Sigma^{-1} \mathbf{y}}{1 + \frac{\mathbf{y}^T \Sigma^{-1} \mathbf{y}}{(1+\zeta)^2}} \right) \ln(1 + \zeta) \\ &\quad - \frac{3}{2} \ln \left(\frac{1 + \mathbf{y}^T \Sigma^{-1} \mathbf{y}}{1 + \frac{\mathbf{y}^T \Sigma^{-1} \mathbf{y}}{(1-\zeta)^2}} \right) \ln(1 - \zeta) \end{aligned} \quad (\text{A.8})$$

$$\begin{aligned} \mu_{g_1} \mu_{g_2} &= \frac{-3}{2} [\ln(1 + \zeta) + \ln(1 - \zeta)] \\ &\quad \cdot \ln \frac{(1 + \mathbf{y}^T \Sigma^{-1} \mathbf{y})^2}{\left(1 + \frac{\mathbf{y}^T \Sigma^{-1} \mathbf{y}}{(1+\zeta)^2}\right) \left(1 + \frac{\mathbf{y}^T \Sigma^{-1} \mathbf{y}}{(1-\zeta)^2}\right)}. \end{aligned} \quad (\text{A.9})$$

Substituting (A.6)–(A.9) into (A.3) and after some mathematical manipulations, the final expression for the variance, as given by (9), can be obtained. In a similar manner, the mean and variance of the log-likelihood ratio under hypothesis H_1 can be obtained.

REFERENCES

- [1] M. Barni, F. Bartolini, and A. Piva, "Multichannel watermarking of color images," *IEEE Trans. Circuits Syst. Video Technol.*, vol. 12, no. 3, pp. 142–156, Mar. 2002.
- [2] T. Tsui, X. Zhang, and D. Androutsos, "Color image watermarking using multidimensional Fourier transforms," *IEEE Trans. Inf. Forensics Security*, vol. 3, no. 1, pp. 16–28, Mar. 2008.
- [3] X. Wang, C. Wang, H. Yang, and P. Niu, "A robust blind color image watermarking in quaternion Fourier transform domain," *J. Syst. Softw.*, vol. 86, no. 2, pp. 255–277, Feb. 2013.
- [4] B. Chen *et al.*, "Full 4-D quaternion discrete Fourier transform based watermarking for color images," *Digit. Signal Process.*, vol. 28, pp. 106–119, May 2014.
- [5] E. Tsougenis, G. Papakostas, D. Koulouriotis, and E. Karakasis, "Adaptive color image watermarking by the use of quaternion image moments," *Exp. Syst. Appl.*, vol. 41, no. 14, pp. 6408–6418, Oct. 2014.
- [6] K. Liu, "Wavelet-based watermarking for color images via visual masking," *Int. J. Electron. Commun.*, vol. 64, no. 2, pp. 112–124, Feb. 2010.
- [7] R. Naskar and R. S. Chakraborty, "Histogram-bin-shifting based reversible watermarking for color images," *IET Image Process.*, vol. 7, no. 2, pp. 99–110, Mar. 2013.
- [8] H. Sadreazami, M. O. Ahmad, and M. N. S. Swamy, "Contourlet domain image modeling by using the alpha-stable family of distributions," in *Proc. IEEE ISCAS*, 2014, pp. 1288–1291.
- [9] J. Hernandez, M. Amado, and F. P. Gonzalez, "DCT-domain watermarking techniques for still images: Detector performance analysis and a few structure," *IEEE Trans. Image Process.*, vol. 9, no. 1, pp. 55–68, Jan. 2000.
- [10] R. Kwitt, P. Meerwald, and A. Uhl, "Color-image watermarking using multivariate power-exponential distribution," in *Proc. 16th IEEE ICIP*, 2009, pp. 4245–4248.
- [11] M. N. Do and M. Vetterli, "The contourlet transform: An efficient directional multiresolution image representation," *IEEE Trans. Image Process.*, vol. 14, no. 12, pp. 2091–2106, Dec. 2005.
- [12] I. J. Cox, M. L. Miller, and J. A. Bloom, *Digital Watermarking*. San Mateo, CA, USA: Morgan Kaufmann, 2001.
- [13] H. Sadreazami, M. O. Ahmad, and M. N. S. Swamy, "A study of multiplicative watermark detection in the contourlet domain using alpha-stable distributions," *IEEE Trans. Image Process.*, vol. 23, no. 10, pp. 4348–4360, Oct. 2014.
- [14] S. Nadarajah and S. Kotz, "Estimation methods for the multivariate t-distribution," *Int. J. Appl. Math. Appl.*, vol. 102, no. 1, pp. 99–118, May 2008.